



Modeling and Simulation of the Drivetrain of a Metal Lathe

Eduardo Paiva Okabe^(✉) and Daniel Iwao Suyama

School of Applied Sciences, University of Campinas - UNICAMP,
PO Box 1068, Limeira, Brazil
{eduardo.okabe,daniel.suyama}@fca.unicamp.br

Abstract. Vibrations in turning machining are one of the most common sources of problems. Bad quality finishing, decrease of the tool life, dimensional errors, and noise are some of the issues generated by these vibrations. To understand the role of each component, this work presents a model of a metal lathe including its drivetrain, and simulates it during the internal turning operation. The drivetrain is composed by an electric motor connected to the spindle through a pulley and belt transmission. The spindle was modeled as a rotor supported by rolling bearings, while the chuck with jaws and the workpiece were considered to be rigidly attached to the spindle. The interface between the workpiece and the tool was modeled considering their relative displacement and the machining condition, thus generating a set of cutting and drag forces that varies during the operation. The tool holder was modeled by three-node finite volume beam elements that are attached to the turret. The turret was connected to the machine frame through a total joint (configured as prismatic). This model was implemented in the dynamic simulation software MBDyn and a module was developed in C++ to mimic the interaction between workpiece and tool. Different configurations of the machine were tested, such as the diameter of the tool holder and the rotation speed of the spindle, and their influence on the drivetrain is reported.

Keywords: Metal lathe · Drivetrain vibrations · Multibody dynamics

1 Introduction

Machining is one of the most important manufacturing process in the metal-work industry. Operations like turning, milling, drilling, and grinding lead to the achievement of pre-established form, dimension, and surface finish of a part. Turning is a relatively fast, precise and cheap operation, which renders it the one of the most effective ways to produce mechanical cylindrical components. However, machining processes usually relies on rotating parts that are subjected to a large variety of vibration phenomena. These vibrations are one of the most common sources of problems, causing bad quality finishing, decrease of the tool life, dimensional errors and noise [15].

The drivetrain of a machining equipment is one of its main components, because most of the power required to cut metal flows through it. The drivetrain is composed by an electric motor connected to the spindle through a pulley/belt transmission. To understand its behavior this work presents a model of a metal lathe and simulates it during the internal turning process, also known as boring operation.

The spindle is the main component of the drivetrain of any machining equipment. Usually being one slender rotating shaft, it brings all sorts of vibration problems, which is exactly the opposite of what its function demands. Aini et al. [1] modeled a grinding machine spindle as a rigid shaft supported by angular contact ball bearings. They studied the effect of the radial force, spindle speed, frictional damping and thrust loads. In their simulations, they discovered that the axial mode was less than half of the frequency of the radial modes and the behavior of the spindle was influenced by the preload in the bearings.

Mannan et al. [11] also studied the vibration on a grinding machine, but they focused on the torsional vibrations. They used a simple three degrees of freedom model to represent workpiece, wheel and spindle. They concluded that the width of cut can lead to the torsional instability of the system due to chatter. Altintas and Weck [2] made a review of the modeling of chatter in metal cutting and grinding processes. They highlighted that although the boring bar is the most flexible part of the hole enlargement process, other parts such as the shaft, chuck and the tool holder can lead to chatter.

Ertürk et al. [6] proposed an analytical model of the spindle-tool dynamics of a drilling machine. They modeled the spindle as a discretized beam using the Timoshenko beam model, with the spindle supported by elastic bearings. The FRF (frequency response function) of the tool generated by the proposal model was compared to the response obtained from a commercial finite element software. They presented a good agreement. Due to the geometry of the drilling machine spindle they showed that the Euler-Bernoulli beam could lead to inaccurate results at high frequencies when compared to the Timoshenko beam.

Roukema and Altintas [13] presented a time domain model of a drilling operation to study the torsional-axial chatter vibrations. The cutting force was calculated by a mechanistic model that uses the feedrate, depth of cut and drill geometry to determine the torque and thrust on the tool. The simulation also considers the generated surfaces to predict the occurrence of vibration phenomena such as chatter. The simulated results were close to the experimental ones, although the authors point out that the process damping would be required to predict the stability of the drilling operation.

Guo et al. [8] analyzed a lathe spindle system under the influence of an unbalanced workpiece. They developed a pure torsional lumped mass system to model the geared drivetrain. The authors concluded that the spindle can not operate at same speed of its natural frequencies because of the instability generated by the unbalance of the chosen workpiece, a crankshaft.

In the next section the methodology adopted to develop the computational model of the metal lathe using a multibody dynamics approach as well as the details of the cutting force calculation are presented.

2 Methodology

The metal lathe can be considered a mechanical constrained system, which can be formulated as a system of Differential-Algebraic Equations (DAE) [12]:

$$\begin{aligned}
 \mathbf{M}\dot{\mathbf{q}} - \boldsymbol{\beta} &= \mathbf{0} \\
 \dot{\boldsymbol{\beta}} + \left(\frac{\partial\boldsymbol{\phi}}{\partial\mathbf{q}}\right)^T \boldsymbol{\lambda}_\phi + \left(\frac{\partial\boldsymbol{\psi}}{\partial\dot{\mathbf{q}}}\right)^T \boldsymbol{\lambda}_\psi &= \sum \mathbf{f}(\mathbf{q}, \dot{\mathbf{q}}, t) \\
 \boldsymbol{\phi}(\mathbf{q}, t) &= \mathbf{0} \\
 \boldsymbol{\psi}(\mathbf{q}, \dot{\mathbf{q}}, t) &= \mathbf{0}
 \end{aligned} \tag{1}$$

where \mathbf{M} is the inertia matrix, $\boldsymbol{\beta}$ is the momentum vector, \mathbf{q} is the position vector, $\boldsymbol{\phi}$ is the system of holonomic constraint equations, $\boldsymbol{\psi}$ is the system of non-holonomic constraint equations, $\boldsymbol{\lambda}_\phi$ is the Lagrange multiplier associated with the holonomic constraints, $\boldsymbol{\lambda}_\psi$ is the Lagrange multiplier associated with the non-holonomic constraints, \mathbf{f} is the vector of external loads, and (\clubsuit) represents the time derivative of (\clubsuit) .

This formulation is implemented in the open source software MBDyn, which is a multiphysics platform that can simulate complex systems. The models on MBDyn are based on nodes, like the ones used on finite element softwares. Nodes provide degrees of freedom, and they can be associated to different physical domains, such as mechanical, thermal and electrical. This structure makes easier to integrate different components of the same machine in one simulation.

Constraints and forces have to be applied on nodes, thus they become part of the modeled system. This is performed by adding two sets of equations to variables associated with each node. The first set is used in the assembly of the system of Eq. (1), and the second set is used during the nonlinear solution phase, if it is necessary.

New elements can be created to compose the model by adding new modules to MBDyn. These modules are written in C++, and they basically contain the system of equations that model the dynamic behavior of the element and its Jacobian matrix. These modules are compiled with MBDyn, and they become part of the software which enable the use of this new element in any model.

The next section presents the set of equations that model the cutting forces in the turning process, which were implemented in a module of MBDyn to compose the complete model of the lathe drivetrain.

2.1 Cutting Model

Using the geometry represented in Fig. 1 it is possible to reproduce the behavior of the cutting process using a semi-analytical model that relates one node fixed to the tool holder (Node 1) and one node attached to the workpiece (Node 2). The

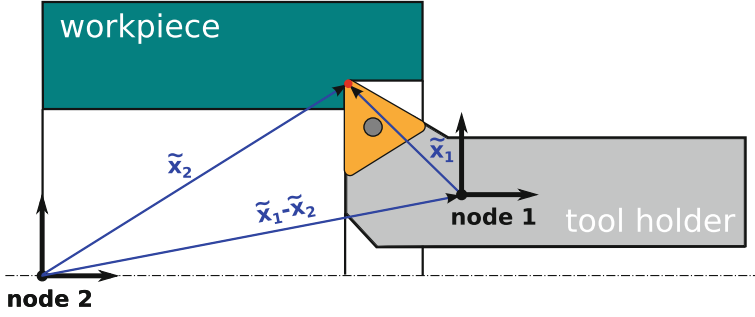


Fig. 1. Geometry of the cutting model.

tool (insert) is considered to be rigidly attached to the tool holder. The kinematic relationship between nodes 1 and 2 is used to calculate the forces through the cutting model, then these forces are transformed to the absolute coordinates and applied to each one of the nodes. The calculation of the moments generated by these forces should consider the point of application of the cutting force, which moves during the machining process. The forces and moments applied to both nodes can be calculated by:

$$\begin{aligned}
 \mathbf{f}_1 &= -\mathbf{R}_{1r}\mathbf{f}_{\text{cut}} \\
 \mathbf{f}_2 &= \mathbf{R}_{1r}\mathbf{f}_{\text{cut}} \\
 \mathbf{c}_1 &= -\mathbf{R}_1\tilde{\mathbf{x}}_1 \times \mathbf{R}_{1r}\mathbf{f}_{\text{cut}} - \mathbf{R}_{1r}\mathbf{c}_{\text{cut}} \\
 \mathbf{c}_2 &= \mathbf{R}_2\tilde{\mathbf{x}}_2 \times \mathbf{R}_{1r}\mathbf{f}_{\text{cut}} + \mathbf{R}_{1r}\mathbf{c}_{\text{cut}}
 \end{aligned} \tag{2}$$

where \mathbf{f}_1 and \mathbf{f}_2 are the forces applied to nodes 1 and 2, \mathbf{c}_1 and \mathbf{c}_2 are the moments applied to nodes 1 and 2, $\mathbf{R}_{1r} = \mathbf{R}_1\tilde{\mathbf{R}}_1$ is the rotation matrix of the tool edge, \mathbf{R}_1 is the rotation matrix of the tool holder node, and $\tilde{\mathbf{R}}_1$ is the rotation matrix of tool edge in relation to the node of the tool holder (node 1), $\tilde{\mathbf{x}}_1$ is the offset between the tool holder node and the cutting edge, and $\tilde{\mathbf{x}}_2$ is the offset between the cutting edge and the node attached to the workpiece, \mathbf{f}_{cut} and \mathbf{c}_{cut} are the cutting force and moment. The calculation of cutting force \mathbf{f}_{cut} was adapted from the model proposed by Xiao et al. [17] to the multibody environment. They based their model on the analytical approach developed by Tarnag et al. [16], but instead of using an analytical formulation, they obtained the cutting properties (shear and friction angles, and shear stress) from the data reported by Kashimura [10].

The cutting force is calculated using the following equation:

$$\begin{aligned}
 F_c &= R \cos(\lambda - \alpha) \\
 F_t &= R \sin(\lambda - \alpha) \\
 R &= \frac{k_{ab}t_1w}{\sin \phi \cos(\phi + \lambda - \alpha)} U(t_1) \\
 \mathbf{f}_{\text{cut}} &= \{0 \quad -F_t \quad -F_c\}^T
 \end{aligned} \tag{3}$$

where R is the cutting force magnitude, λ is the friction angle, α is the rake angle, k_{ab} is the shear stress, t_1 is the chip thickness, w is the cutting width, and $U(t_1)$ is the unit step, which is zero unless t_1 is positive. Using the experimental data reported by Kashimura [10] for the S45C carbon steel, the shear angle, the friction angle and the shear stress become:

$$\begin{aligned}\phi &= \exp(0.0587v + 1.0398t_1 + 0.6742\alpha - 1.2392) \\ \lambda &= \exp(-0.0546v - 0.8856t_1 + 0.8923\alpha - 0.2388) \\ k_{ab} &= \exp(0.0059v - 0.4246t_1 + 0.0818\alpha + 6.3211)\end{aligned}\quad (4)$$

where v is the cutting speed. The dynamic variables of the cutting model must be calculated using the relative motion between the tool edge and the workpiece:

$$\begin{aligned}\mathbf{x}_{rel} &= \mathbf{R}_1 \tilde{\mathbf{x}}_1 + \mathbf{x}_1 - \mathbf{x}_2; \\ \boldsymbol{\omega}_{rel} &= \mathbf{R}_{1r}^T (\boldsymbol{\omega}_2 - \boldsymbol{\omega}_1) \\ \dot{\mathbf{x}}_{rel} &= \dot{\mathbf{x}}_1 + \boldsymbol{\omega}_1 \times \mathbf{R}_1 \tilde{\mathbf{x}}_1 - \dot{\mathbf{x}}_2\end{aligned}\quad (5)$$

where \mathbf{x}_1 is the position of the tool holder node, \mathbf{x}_2 is the position of the workpiece node, $\boldsymbol{\omega}_{rel}$ is the relative angular velocity between the tool and the workpiece, $\boldsymbol{\omega}_1$ and $\boldsymbol{\omega}_2$ are the angular velocity of the nodes associated to the tool (node 1) and workpiece (node 2), $\dot{\mathbf{x}}_{rel}$ is the relative linear velocity, $\dot{\mathbf{x}}_1$ and $\dot{\mathbf{x}}_2$ are the linear velocities of the nodes 1 and 2.

Equation 5 provides the information to determine the dynamic variables of the cutting model:

$$\begin{aligned}w &= (x_{feed} - \mathbf{x}_{rel}[x]) \cdot 10^3 \\ t1 &= (\sqrt{\mathbf{x}_{rel}[y]^2 + \mathbf{x}_{rel}[z]^2} - r) \cdot 10^3 \\ v &= -\boldsymbol{\omega}_{rel}[x] \cdot r \\ \dot{y} &= \frac{\mathbf{x}_{rel}[y] \cdot \dot{\mathbf{x}}_{rel}[y] + \mathbf{x}_{rel}[z] \cdot \dot{\mathbf{x}}_{rel}[z]}{\sqrt{\mathbf{x}_{rel}[y]^2 + \mathbf{x}_{rel}[z]^2}} \\ \alpha &= \alpha_0 - \arctan\left(\frac{\dot{y}}{v}\right) - \arctan\left(\frac{\mathbf{x}_{rel}[y]}{\mathbf{x}_{rel}[z]}\right)\end{aligned}\quad (6)$$

where x_{feed} is a function which determines the tool feed [4], the brackets $[i]$ indicates that the i^{th} component of the vector (for instance, $\mathbf{x}_{rel}[x]$ refers to the x component of the position vector \mathbf{x}_{rel}), r is the radius of the workpiece, α_0 is the initial rake angle.

This formulation was implemented on the MBDyn as an element through a module written in C++. Once compiled this element could be included in the metal lathe model.

3 Metal Lathe Modeling

Although the cutting model is essential to model the dynamic behavior of a metal lathe, the interaction between workpiece and tool is just one of the elements of

the model. Figure 2 shows an outline of the metal lathe modeled in this work with the coordinate system adopted, which is not the usual coordinate system seen in machining research, where the X-axis would be in the place of the Y-axis of Fig. 2.

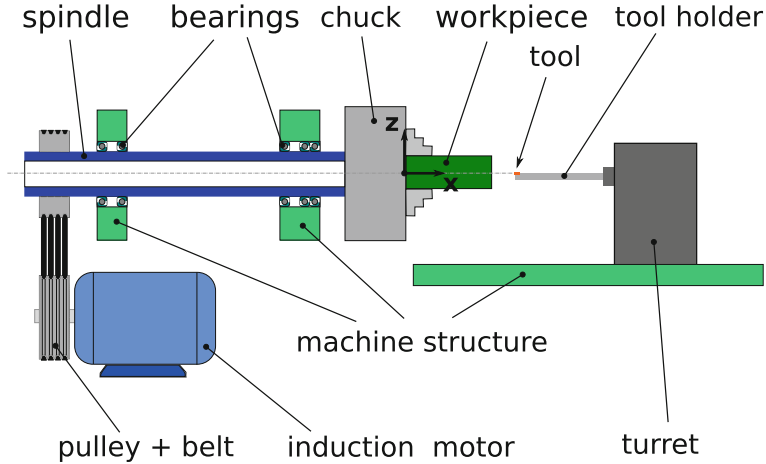


Fig. 2. Outline of the metal lathe and its coordinate system.

The spindle was modeled as discretized beam elements that uses the finite volume formulation proposed by Ghiringhelli et al. [7]. It is a large displacement slender beam that is computationally efficient and can be easily integrated in multibody models. This element is composed by three nodes that are directly related to the dynamic nodes of MBDyn.

The spindle is supported by five ball bearings that were represented by the nonlinear model proposed by Gargiulo as reported by Hambric et al. [9]. This configuration renders the support of the spindle extremely stiff, which is desirable to keep the precision of the cutting process even under heavy load machining.

One of the ends of the spindle is connected to an induction motor through a pulley-belt system. This motor was modeled using the formulation proposed by Dresig and Holzweißig [5] to represent an asynchronous motor. This element was implemented by Reinhard Resch in the MBDyn and it simplifies the electromagnetic equation expressing the dynamic behavior of the motor through only three variables: slippage, breakdown slippage and breakdown torque.

The pulley-belt system was modeled using an elastic rod element that represents the tension applied by the belts to both pulleys and a deformable axial joint (torsional spring) that transmits the rotation from the motor rotor to the spindle. The stiffness and damping properties of the belt were determined using the experimental data presented by Shangguan and Zeng [14] and Čepón et al. [3].

The chuck and the workpiece were modeled as rigid bodies that are rigidly attached to the spindle end node. The turret was also modeled as a rigid body that supports the tool holder and moves along the X-axis.

The tool holder was modeled as a discretized finite volume beams like the spindle. Internal turning is known to cause vibration problems during machining, due to the cantilever geometry of the tool holder, which is a slender beam with a tool in the tip.

Finally the holder head and tool itself (insert) were modeled as a rigid body attached to the other end of the holder.

The model has 28 structural nodes and each node has 6 d.o.f. (degrees of freedom). Thus the model has a total of 168 d.o.f. of which 116 are constrained by the algebraic equations (Eq. 1). The integration method of MBDyn is a A/L linear multistep algorithm [12] with a constant time step of 1×10^{-4} s (or a sampling frequency equals to 10 kHz).

The system is completely static in the initial time only subjected to the gravity force. The electric motor accelerates the spindle to a defined speed and then the turret moves to start the machining process.

Table 1 summarizes the parameters used in the simulation of the lathe.

4 Results

To verify the dynamic behavior of the lathe, it was simulated in six different conditions. The influence of the flexibility of the tool holder (boring bar) was verified by using two different diameters: 16 and 20 mm. They were tested under two rotation speeds: 1000 rpm (132 m/min) and 2000 rpm (264 m/min), so the cutting force could be tested under different cutting speeds. To give a realistic excitation source vibration for the system, the workpiece radius is considered to have a random variation with an amplitude of 0.1 mm.

The last two tests were used to check the effect of the chatter on the drivetrain. To mimic this behavior, a sine function with an amplitude of 0.1 mm was added to the workpiece radius. This sine function has a frequency of 650 Hz, which is close to the vibration frequency of the tool holder during the machining process. Figure 3 shows the power spectral density of the angular velocity of the chuck before the tool starts to machine the workpiece (left) and during the machining (right). Before the cutting a peak around 35 Hz can be seen on all simulated situations, which is associated to the first mode of the drivetrain system (motor, belt and spindle). That vibration comes from the fast acceleration of the spindle imposed by the motor. This peak decreases when the machining takes place, however, another peak shows up at 585 Hz related to the first flexural mode of the tool holder. Even though the frequency associated to this mode is different from the 16 mm to 20 mm tool holder, the peaks occur at the same frequency.

Another information that can be extracted from Fig. 3 is that the diameter of the tool holder had a greater influence on the angular velocity of the chuck than the increase of the rotation speed itself. In the opposite end of the spindle

Table 1. Lathe model parameters

Part	Parameter	Value
Induction motor	Slippage	0.1
	Breakdown torque	58.83 Nm
	Viscous damping	0.0015
	Rotation speed	1000 and 2000 rpm
Tool holder	Length	125 mm
	Diameter	16/20 mm
	Material	steel
Spindle	External diameter	75 mm
	Internal diameter	40 mm
	Length	567 mm
	Material	Steel
Ball bearings	Sphere diameter	11 mm
	Number of spheres	22
	Contact angle	25°
Chuck	Length	80 mm
	Mass	14.25 kg
	Moment of inertia I _{xx}	0.051 kg·m ²
	Moment of inertia I _{yy} , I _{zz}	0.033 kg·m ²
Workpiece	Mass	1 kg
	Moment of inertia I _{xx}	1·10 ⁻⁶ kg·m ²
	Moment of inertia I _{yy} , I _{zz}	8·10 ⁻⁶ kg·m ²
	Internal diameter	40 mm
	Material	steel S45C
Cutting properties	Speed	132 and 264 m/min
	Feedrate	0.1 mm/rev
	Rake angle	3°
Pulley-belt	Transmission ratio	1:1

there is the pulley set which is connected to the motor. Its angular velocity can be seen on Fig. 4 and the same behavior is observed although the second peak has a lower frequency (~ 500 Hz) and it is more damped. Figure 5 shows that the influence of the tool holder is much less pronounced in the motor than the spindle (Fig. 4), which means that the belt is filtering the vibration coming from the spindle. Another point to be observed is that the vibration power of the mode related to the drivetrain is largely reduced during the machining, which means that the cutting process effectively constrains the torsional motion of the spindle.

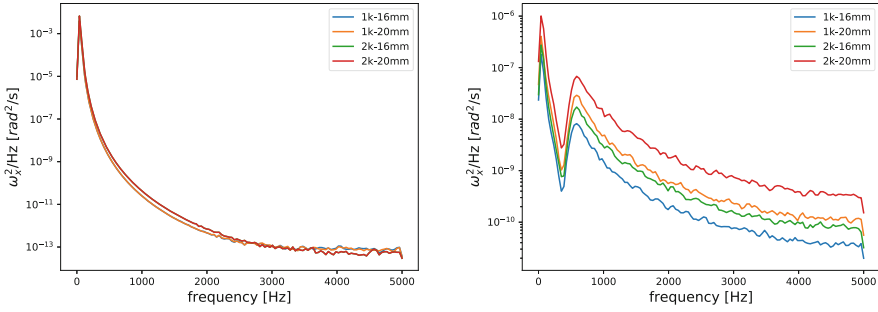


Fig. 3. Power spectral density of the angular velocity of the chuck before (left) and during machining (right).

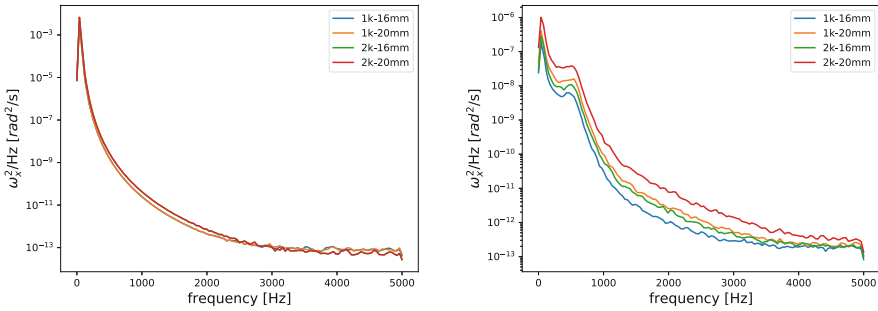


Fig. 4. Power spectral density of the angular velocity of the spindle pulley before (left) and during machining (right).

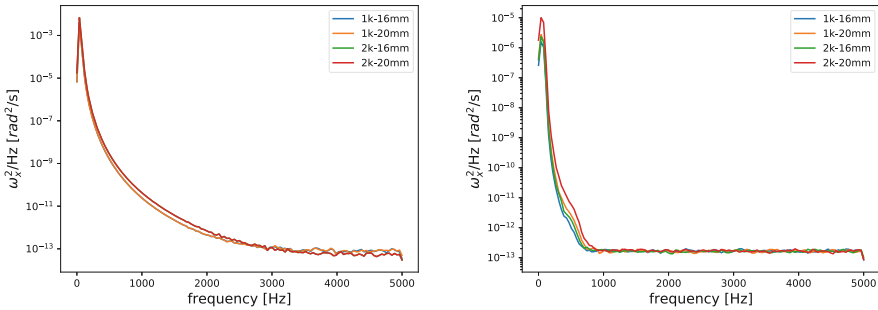


Fig. 5. Power spectral density of the angular velocity of the motor rotor before (left) and during machining (right).

To verify the effect of the drivetrain on the tool, its angular velocity is represented on Fig. 6. While there is a small influence of the tool holder on the motor (Fig. 5), the opposite is not true.

Another phenomenon very interesting to analyze is the chatter, which is more pronounced in the internal machining operation. The chatter is related

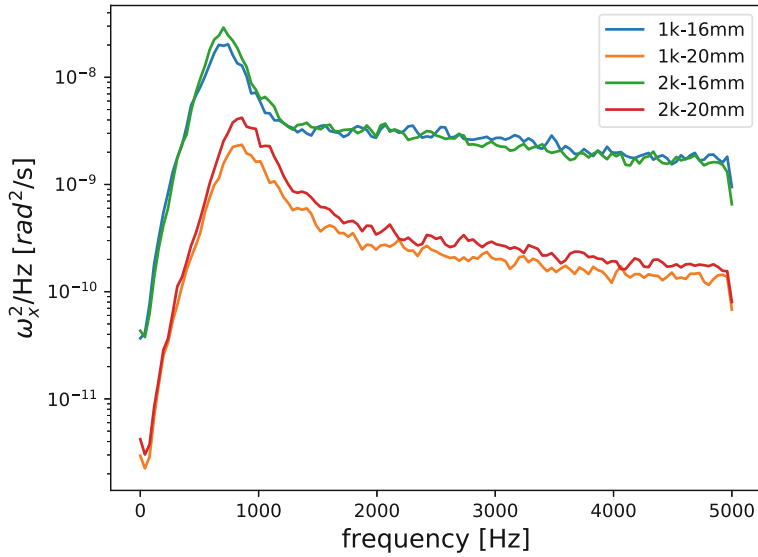


Fig. 6. Power spectral density of the angular velocity of the tool during machining.

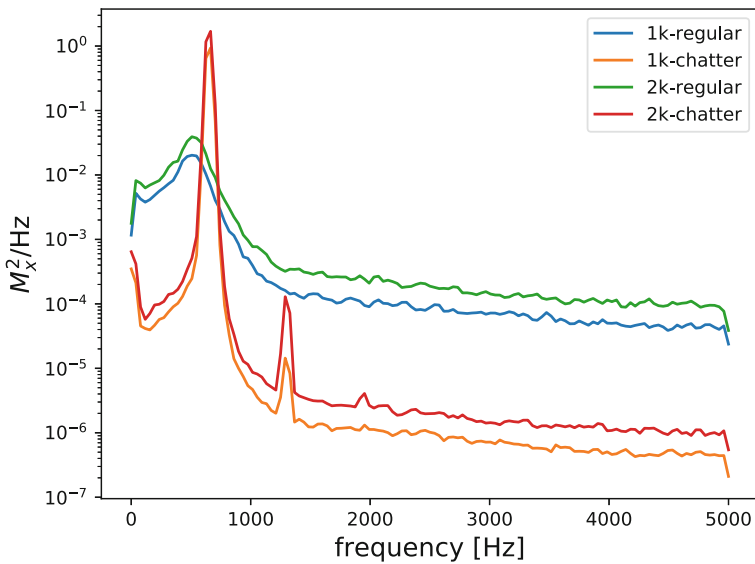


Fig. 7. Power spectral density of the moment applied to the spindle.

to the vibration of the tool holder that is imprinted in the machined surface of the workpiece. When the tool is executing other passes on this surface, the tool holder is excited by the impression left which increases the vibration and deteriorates the surface finish. The chatter phenomenon can decrease the tool

life span and it causes vibration problems on the components of the drivetrain. To simulate the chatter phenomenon, a sine wave was added to the workpiece radius profile with a frequency that matches the flexural mode of the tool holder and amplitude of 0.1 mm.

Figure 7 shows the power spectral density of the moment applied to the spindle through the chuck. The moment due to chatter is much higher than normal cutting operation (without chatter) and there is a second peak on 1285 Hz, which is approximately twice the frequency of the first peak (650 Hz).

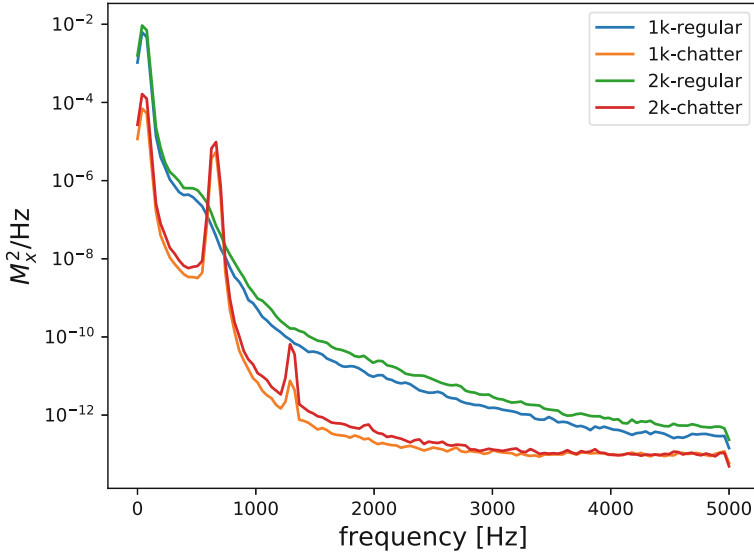


Fig. 8. Power spectral density of the moment applied to the motor.

The vibration caused by the chatter is also present in the moment applied to the motor which can be observed in Fig. 8.

5 Conclusions

A complete model of lathe drivetrain was simulated under machining conditions using a multibody dynamics software, that demonstrated the influence of the cutting process on the torsional vibration of drivetrain components. The internal turning machining was adopted in order to highlight the effect of the flexibility of the tool holder.

Results showed that there is a considerable effect of this flexibility on the spindle behavior, but this effect is filtered by the pulley-belt set to the motor. The vibration of the drivetrain does not seem to affect the tool motion, that is largely influenced by the behavior of the tool holder.

However, the influence of the chatter phenomenon is transmitted through the spindle to the electric motor, which indicates that the vibration generated by it can damage the motor.

References

1. Aini, R., Rahnejat, H., Gohar, R.: A five degrees of freedom analysis of vibrations in precision spindles. *Int. J. Mach. Tools Manuf.* **30**(1), 1–18 (1990)
2. Altintas, Y., Weck, M.: Chatter stability of metal cutting and grinding. *CIRP Ann.-Manuf. Technol.* **53**(2), 619–642 (2004)
3. Čepon, G., Manin, L., Boltežar, M.: Introduction of damping into the flexible multibody belt-drive model: a numerical and experimental investigation. *J. Sound Vib.* **324**(1–2), 283–296 (2009)
4. Diniz, A.E., Marcondes, F.C., Coppini, N.L.: *Tecnologia da usinagem dos materiais*. Artliber Editora (2006)
5. Dresig, H., Holzweiffig, F.: *Dynamics of Machinery: Theory and Applications*. Springer (2010)
6. Ertürk, A., Özgüven, H., Budak, E.: Analytical modeling of spindle-tool dynamics on machine tools using timoshenko beam model and receptance coupling for the prediction of tool point frf. *Int. J. Mach. Tools Manuf.* **46**(15), 1901–1912 (2006)
7. Ghiringhelli, G.L., Masarati, P., Mantegazza, P.: A multibody implementation of finite volume beams. *AIAA J.* **38**(1), 131–138 (2000)
8. Guo, R., Jang, S.H., Choi, Y.H.: Torsional vibration analysis of lathe spindle system with unbalanced workpiece. *J. Central South Univ. Technol.* **18**(1), 171–176 (2011)
9. Hambric, S.A., Shepherd, M.R., Campbell, R.L., Hanford, A.D.: Simulations and measurements of the vibroacoustic effects of replacing rolling element bearings with journal bearings in a simple gearbox. *J. Vib. Acoust.-Trans. ASME* **135**(3) (2013)
10. Kashimura, Y.: Study on prediction of tool flank wear by means of cutting force ratios (1st report). *J. Jpn. Soc. Prec. Eng.* **51**(11), 2115–2121 (1985). (in Japanese)
11. Mannan, M., Fan, W., Stone, B.: The effects of torsional vibration on chatter in grinding. *J. Mater. Process. Technol.* **89**, 303–309 (1999)
12. Masarati, P., Morandini, M., Mantegazza, P.: An efficient formulation for general-purpose multibody/multiphysics analysis. *J. Comput. Nonlinear Dyn.* **9**(4), 041001 (2014)
13. Roukema, J.C., Altintas, Y.: Time domain simulation of torsional-axial vibrations in drilling. *Int. J. Mach. Tools Manuf.* **46**(15), 2073–2085 (2006)
14. Shangquan, W.B., Zeng, X.K.: Modeling and validation of rotational vibration responses for accessory drive systems part i: experiments and belt modeling. *J. Vib. Acoust.* **135**(3), 031002 (2013)
15. Suyama, D., Diniz, A., Pederiva, R.: Tool vibration in internal turning of hardened steel using cBN tool. *Int. J. Adv. Manuf. Technol.* **88**(9–12), 2485–2495 (2017)
16. Tarng, Y., Young, H.T., Lee, B.: An analytical model of chatter vibration in metal cutting. *Int. J. Mach. Tools Manuf.* **34**(2), 183–197 (1994)
17. Xiao, M., Karube, S., Soutome, T., Sato, K.: Analysis of chatter suppression in vibration cutting. *Int. J. Mach. Tools Manuf.* **42**(15), 1677–1685 (2002)